Method for wettability characterization based on contact line pinning

D. I. Dimitrov,[1,2] A. Milchev,[1,3] and K. Binder[1]
[1]*Institut für Physik, Johannes Gutenberg-Universität, D-55099 Mainz, Germany*
[2]*Inorganic Chemistry and Physical Chemistry Department, University of Food Technology, Maritza Boulevard 26, 4000 Plovdiv, Bulgaria*
[3]*Institute of Physical Chemistry, Bulgarian Academy of Sciences, 1113 Sofia, Bulgaria*
(Received 12 January 2010; published 7 April 2010)

We demonstrate an efficient and reliable method for wettability characterization by determining the contact angle θ which a liquid-vapor interface makes with a solid wall. The purpose is to overcome the difficulties, related to the curvature of the liquid-vapor interface, which make measurements of θ rather uncertain, especially on the micro- and nanoscale. The method employs a specially designed slitlike channel in contact with a reservoir whereby the wettability of one of the slit walls is to be examined whereas the other (auxiliary) wall is separated by half into a lyophilic and a lyophobic part so as to pin the incoming fluid and fix the one end of the liquid-vapor interface. In the present work, the physical background of the method is elucidated theoretically while the method's applicability is demonstrated by molecular-dynamics simulation of a typical Lennard-Jones fluid, in contact with an atomistic wall. The wettability of the latter, as described by the corresponding contact angle θ, is accurately determined by variation of the liquid-wall interaction in a very broad interval.

DOI: 10.1103/PhysRevE.81.041603 PACS number(s): 68.08.Bc, 68.03.Hj, 05.70.Np, 07.05.Tp

I. INTRODUCTION

The contact angle θ between a liquid droplet and a solid substrate under incomplete wetting conditions [1–9] is a basic quantity needed for the interpretation of many physical phenomena (droplet motion [2,9–14], filling of capillaries [15–20], boundary conditions for nanofluidics [21–28], heterogeneous nucleation in supersaturated vapors [29–32], etc.). Although Young's equation [33] that describes the balance of surface-tension forces at the contact line is known since more than 200 years ago,

$$\gamma_{WV} - \gamma_{LW} = \gamma_{LV} \cos\,\theta, \tag{1}$$

(here and in what follows, γ_{WV}, γ_{LW}, and γ_{LV} are the wall-vapor, wall-liquid, and liquid-vapor interfacial tensions, respectively) accurate measurements of contact angles remain still a problem, in particular if one is interested in droplets on micro- and nanoscales. The problem with reliable estimation of contact angles is also a standard one in computer simulations of different model fluids. Both in real experiments [9,34] and in computer simulations [35–41], one usually measures the angle between a tangent plane to the droplet surface and the plane of the substrate. Such a measurement, however, is frequently cumbersome [37,38] due to interface curvature and possible effects of line tension τ [42–51] which invalidates Eq. (1) since then the contact angle is given by

$$\gamma_{WV} - \gamma_{LW} + \frac{\tau}{r} = \gamma_{LV} \cos\,\theta, \tag{2}$$

assuming that the contact line is a circle of radius r. Estimation of line tension from experiment and/or theory and simulation has remained a controversial subject until today [32,51,52]. Moreover, when one deals with droplets on micro- and nanoscales, additional problems arise due to the poor smoothness of the density profile between liquid and vapor, the droplet surface can no longer be viewed as an infinitely thin membrane for the length scales of interest [1–9], and also the contact line is smeared out. If one works close to conditions of critical wetting, the curved liquid-vapor interface of the droplet then gradually bends over to a thin liquid film at the substrate which acts as a precursor to the wetting layer [53]. Under such conditions, geometrical constructions of a tangent plane to the droplet surface are quite ambiguous and quantitatively unreliable.

In the present work, we suggest a convenient setup which overcomes the aforementioned difficulties and permits an accurate and reliable measurement of the contact angle at various (chemically decorated, polymer-brush coated, solid rough, etc.) surfaces. Within the framework of the method, one determines the contact angle θ between the flat liquid-vapor interface and the surface of concern in a specially designed slit connected to a reservoir. The role of the reservoir is to eliminate any curvature-induced Laplace pressure in the fluid and, therefore, guarantee the existence of a *flat* liquid-vapor interface. This is achieved by pinning the interface to a fixed line of triple contact on the opposite (auxiliary) wall while allowing free motion of the other triple contact line along the plane of concern (Fig. 1). In our setup, we fix the triple contact line as the line of separation between a lyophilic half of the wall, adjacent to the reservoir, and a lyophobic half which repels the fluid. As far as different contact angles imply different amounts of liquid in the slit, a free exchange of liquid between slit and reservoir is essential. Clearly, the reservoir should contain sufficient amount of liquid so that the slit is filled as much as required while still a freely moving liquid-vapor interface in the reservoir is maintained.

The fixed position of the line of triple contact on the pinning wall makes the triple contact on the wall of interest (for a sufficiently broad slit or a system with periodic boundary conditions) also a straight line whose length does not depend on θ. The latter guarantees no line tension effects on the measured contact angles and therefore a significant advantage as compared to θ measurements in droplets. We believe that the suggested setup may be conveniently used in both real experiments and computer simulations whereby the par-

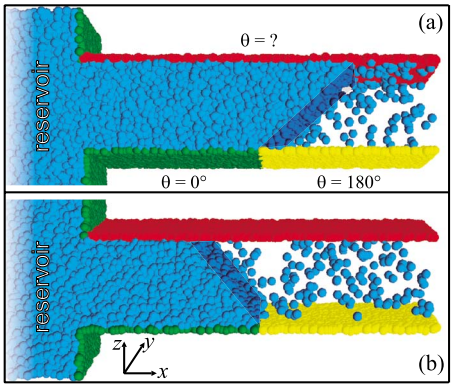

FIG. 1. (Color online) Snapshots of two equilibrium configurations of a fluid [blue (medium gray)] particle in a flat slit connected to a reservoir. The pinning line separates the lyophilic [green (gray)] from the lyophobic [yellow (light gray)] sections of the lower wall. Predominantly (a) wettable and (b) nonwettable upper walls in red (dark gray) show two distinct well-defined contact angles with almost flat liquid-vapor interfaces.

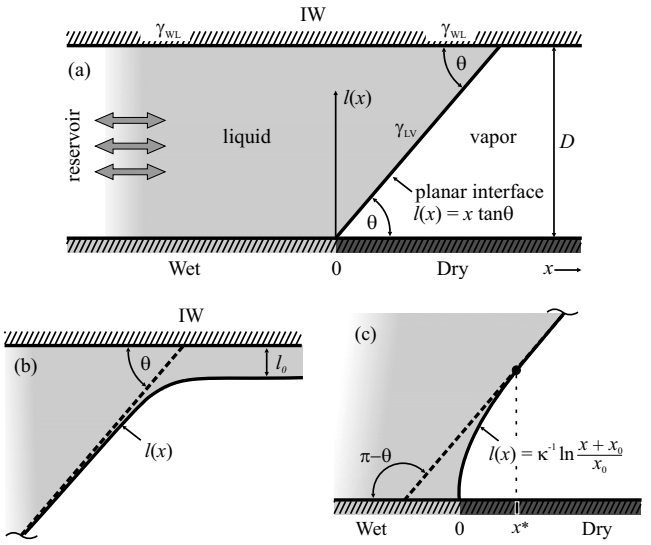

FIG. 2. Schematic presentation of the liquid-vapor interface in a slit.

ticular kind of simulation algorithm should be irrelevant.

The physical justification of the present method is briefly outlined in Sec. II where we also demonstrate analytically that small-scale (mesoscopic) corrections to our macroscopic-scale arguments for the existence of flat phase boundaries in the proposed setup may safely be ignored. The setup itself and the model used in our computer experiment are described in Sec. III. In Sec. IV, we present data from our molecular-dynamics (MD) simulation and produce a calibration relationship between any chosen strength of the liquid-wall interaction and the resulting contact angle θ. We conclude then in Sec. V with a brief summary of the suggested method.

II. THEORETICAL BACKGROUND

We consider a thin-film geometry with two infinite parallel planes apart at (macroscopic) distance D in z direction. The slit contains a fluid at liquid-vapor coexistence. At the upper wall, we assume incomplete wetting (IW) conditions so that the planar liquid-vapor interface forms a contact angle θ with θ being given by the Young equation [Eq. (1)].

The lower (xy plane at $z=0$) plane is chemically heterogeneous, such that the half plane $x<0$ along the y axis ($x=0$) wets the fluid (with contact angle $\theta=0$) whereas the half plane $x>0$ is lyophobic (i.e., prefers the vapor) with $\theta=\pi$. Of course, even when we describe the scale as "microscopic," we assume that D is still small enough so that gravity effects may be safely neglected. On the scales accessible to molecular-dynamics simulations, this condition certainly holds.

Then, on macroscopic scales, the liquid-vapor interface will be effectively pinned along the y axis at $x=0$, provided liquid-vapor coexistence in the thin film is considered. This interface will meet the other (homogeneous) wall at angle θ. If curvature-induced Laplace pressure is absent, as is the case in our setup due to the special reservoir design, the resulting macroscopic picture will be that of a planar interface, starting at $x=0$ on the lower wall and ending at $x=D\tan(\frac{\pi}{2}-\theta)$ on the upper wall. For simplicity, we shall consider only short-range forces between the fluid particles and the wall.

On *mesoscopic* scale, one expects to see some deviations from the macroscopic picture in the vicinity of the contact lines, of course [see Figs. 2(b) and 2(c)]. These deviations are particularly pronounced for small θ. In the case of a second-order wetting transition, the vapor phase forms then a liquid layer of thickness l_0 (as a precursor of a wetting layer) along the upper wall, as shown in Fig. 2(b). Close to the contact line, a gradual crossover from the region of constant distance l_0 to the inclined interface plane, described by $l(x)=x\tan\theta$, takes place. Similarly, near the chemical heterogeneity, the interface deviation from a simple plane follows a logarithmic behavior [54], $l(x)=\kappa^{-1}\ln[(x+x_0)/x_0]$ for $x<x^*$, where κ^{-1}, x_0 are constants characterizing the interface in terms of effective interface Hamiltonian (see below). The constant x^*, where the logarithmic curve meets the straight line, is defined by the condition $dl/dx=\tan\theta$.

Of course, this description of the interface is approximate in many aspects: capillary-wave broadening of the interface is ignored and the "intrinsic" thickness is neglected as well. Likewise, no attention is paid to phenomena on the atomistic scale (fluid layering close to the walls, detailed structure of the contact lines, etc.) Therefore, it is necessary to address the conditions under which this approximate theory holds.

The problem when a fluid-vapor interface meets a heterogeneously structured substrate, as in Fig. 2(a), was considered earlier by Parry *et al.* [54] for the case of short-range surface potentials. The effective Hamiltonian [2–8] is

$$\mathcal{H}\{l(x)\}=\int dx\left[\gamma_{LV}\sqrt{1+\left(\frac{dl}{dx}\right)^2}+V_{eff}(l)\right]. \qquad (3)$$

In Eq. (3), $V_{eff}(l)$ denotes a local position-dependent binding potential. In what follows, we discuss only the case of small contact angles $\theta\ll 1$ so as to compare to treatments in the

literature. Then, the square root in Eq. (3) may be expanded and, omitting a constant, one finds

$$\mathcal{H}\{l(x)\} = \int dx \left[\frac{\gamma_{LV}}{2} \left(\frac{dl}{dx} \right)^2 + V_{eff}(l) \right], \tag{4}$$

which is solved by the Euler-Lagrange equation

$$\frac{dV_{eff}(l)}{dl} = \gamma_{LV} \frac{d^2 l}{dx^2}. \tag{5}$$

For the case of complete wetting and short-range forces, one simply can take [2–8] $V_{eff}(l) = a \exp(-\kappa l)$, where κ has the meaning of inverse bulk correlation length [56]. The Euler-Lagrange equation can be integrated once to give

$$\left(\frac{dl}{dx} \right)^2 = \frac{2a}{\gamma_{LV}} \exp(-\kappa l) + \text{const.} \tag{6}$$

In the present problem, the integration constant is zero. When taking the root, one should be aware that there are two signs:

$$\frac{dl}{dx} = \pm \sqrt{\frac{2a}{\gamma_{LV}}} \exp\left(-\frac{\kappa l}{2} \right). \tag{7}$$

For the case when at the upper wall $\theta < \pi/2$ [Fig. 2(b)], one has $dl/dx > 0$ while for $\theta > \pi/2$, one should take the solution $dl/dx < 0$. In the first case, one obtains $\kappa(x+x_0) = \sqrt{2\gamma_{LV}/a} \exp(\kappa l/2)$ or

$$\kappa l(x) = 2 \ln \frac{x + x_0}{x_0}, \tag{8}$$

where the constant $x_0 = \kappa^{-1} \sqrt{2\gamma_{LV}/a}$ has been chosen such that $l(x=0)=0$, compatible with Fig. 2(c). Since $dl/dx = 2/[\kappa(x+x_0)]$ should be equal to $\tan\theta$, one can determine the position x^* of the point where the straight-line solution takes over, $x^* + x_0 = 2/[\kappa \tan\theta] \approx 2/\kappa\theta$. Evidently, x^* grows rapidly as $\theta \to 0$. In contrast, the distance l where this crossover occurs increases only as $\ln\theta$,

$$l(x^*) = \frac{2}{\kappa} \ln\left(\frac{\kappa x_0}{2} \tan\theta \right) \approx \frac{2}{\kappa} \ln \frac{\kappa x_0 \theta}{2}. \tag{9}$$

Consider now the wall which is under incomplete wetting conditions. For the case of second-order wetting transition, the effective potential is

$$V_{eff}(l) = a_0 \delta\epsilon \exp(-\kappa l) + b \exp(-2\kappa l), \tag{10}$$

where $\delta\epsilon$ measures the distance from the wetting transition ($\delta\epsilon > 0$ in the IW plane) and a_0, b are constants. For the sake of simplicity, one may ignore the distinction in the range parameter κ of the two walls (κ^{-1} describes the range of the effective wall potential, not the range of intermolecular interactions in the fluid). One finds the parameter l_0 [Fig. 2(b)], from $\partial V_{eff}(l)/\partial l|_{l=l_{\min}} = 0$, that is,

$$l_0 = -\kappa \ln \frac{\delta\epsilon}{2b}. \tag{11}$$

The minimum of the potential itself is related to the contact angle via $V_{eff}(l_0) = -b(\frac{\delta\epsilon a_0}{2b})^2 = \gamma_{LV}(\cos\theta - 1) \approx -\frac{1}{2}\gamma_{LV}\theta^2$ and hence

$$\theta \approx \sqrt{\frac{2b}{\gamma_{LV}}} \left(\frac{\delta\epsilon a_0}{2b} \right). \tag{12}$$

In order to derive an equation for the interface $l(x)$ of the type shown in Fig. 2(b), one may consider the fluid to be for simplicity on the right-hand side at $x > 0$, while for $x \to -\infty$, only a thin liquid layer covers the wall under the vapor phase so that $l(x \to -\infty) = l_0$. Now the first integral of the Euler-Lagrange equation reads

$$\frac{\gamma_{LV}}{2} \left(\frac{dl}{dx} \right)^2 = -a_0 \delta\epsilon \exp(-\kappa l) + b \exp(-2\kappa l) + \text{const.} \tag{13}$$

In order to simplify the boundary condition for $x \to -\infty$, one may take $l = l_0$ and $dl/dx = 0$. For the integration constant, using $\exp(-\kappa l_0) = \delta\epsilon a_0/2b$, this yields simply const $= (\delta\epsilon a_0)^2/4b = \gamma_{LV}(1 - \cos\theta) \approx \frac{1}{2}\gamma_{LV}\theta^2$. As expected, for $x \to \infty$, this equation admits a solution where l gets large and, therefore, the exponentials $\exp(-\kappa l)$, $\exp(-2\kappa l)$ can be neglected so that

$$\frac{dl}{dx} = \theta, \tag{14}$$

as expected from Fig. 2 in the limit of small contact angles assumed here.

Eventually, we consider the case of first-order wetting transition. Then the binding potential $V_{eff}(l)$ needs to be chosen ($b > 0$, $c > 0$) as

$$V_{eff}(l) = -a_0 \delta\epsilon \exp(-\kappa l) - b \exp(-2\kappa l) + c \exp(-3\kappa l). \tag{15}$$

Note the different sign of the term with $\exp(-3\kappa l)$. Choosing again $y = \exp(-\kappa l)$ as variable, the equation $\partial V_{eff}(l)/\partial l|_{l=l_{\min}} = 0$ is solved by

$$y = \exp(-\kappa l_0) = \frac{b}{3c} \pm \sqrt{\left(\frac{b}{3c} \right)^2 + \frac{2\delta\epsilon a_0}{3c}}. \tag{16}$$

Using this solution in $V_{eff}(l)$, one finds $V_{eff}(l_0) < 0$ in the incomplete wetting regime and $V_{eff}(l_0) \approx \frac{1}{2}\gamma_{LV}\theta^2$ if $\theta \ll 1$. The reasoning that for $x \to \infty$ the solution is $dl/dx = \theta$ holds as before. It remains to solve $l(x)$ explicitly, however.

In our treatment, we imply that the solution [Eq. (13)] for $D \to \infty$ can be matched at the point $\{x^*, l(x^*)\}$ in Fig. 2(c) to the solution of the lower wall [Eq. (9)], which amounts to the neglect of terms of order $\exp(-\kappa D)$. Such small terms appear when one deals with Eq. (5) and includes in $V_{eff}(l)$ terms due to both walls together. As far as κ^{-1} is a length of the order of a Lennard-Jones diameter in our simulation, this neglect is justified.

III. MODEL AND SIMULATION ASPECTS

In this work, we verify the method by means of MD simulation of a simple generic model on a coarse-grained level. In our MD simulation (see Fig. 1), the fluid particles interact with each other through a Lennard-Jones (LJ) potential

$$U_{LL}(r) = 4\epsilon_{LL}[(\sigma_{LL}/r)^{12} - (\sigma_{LL}/r)^{6}], \tag{17}$$

where $\epsilon_{LL}=1.4$ and $\sigma_{LL}=1.0$. The diameter σ_{LL} of a particle of the fluid is used as a measure of the length scale in our model.

The same potential [Eq. (17)], albeit with an amplitude ϵ_{LW}, is used for the interaction between particles of the liquid and of the wall. By changing the strength, ϵ_{LW}, one can readily vary the wall wettability between lyophobic [in that case, a truncated and shifted by ϵ_{LW} version of Eq. (17), generally known as Weeks-Chandler-Anderson potential, is used) and entirely lyophilic ($\epsilon_{LW} \approx 1.4$).

The walls of the slit are made of particles forming a triangular lattice with spacing 1.0 in units of the liquid atom diameter σ_{LL}. The wall atoms may fluctuate around their equilibrium positions, subject to a finitely extensible nonlinear elastic (FENE) potential

$$U_{\mathrm{FENE}}(r) = -15\epsilon_W R_0^2 \ln(1 - r^2/R_0^2), \tag{18}$$

with $R_0=1.5$ and $\epsilon_W=1.0k_BT$, where k_B denotes the Boltzmann constant and T is the temperature of the system; r is the distance between the particle and the virtual point which represents its equilibrium position in the wall structure. The FENE-potential acts like an elastic string between the wall particles and their equilibrium positions in the lattice and keeps the structure of the wall densely packed hexagonal. In addition, the wall particles interact with each other via a LJ potential with $\epsilon_{WW}=1.0$ and $\sigma_{WW}=0.8$. This choice of interactions guarantees no penetration of liquid through the wall and at the same time the mobility of the wall particles corresponds to the system temperature.

Molecules are advanced in time via the velocity-Verlet algorithm with integration time step $\delta t=0.01t_0$, where t_0 is the basic MD time unit and we have taken $k_BT=1$. The temperature is maintained by a dissipative-particle-dynamics (DPD) thermostat, with friction parameter $\xi=0.5$, thermostat cutoff $r_c=2.5\sigma_{LL}$, and step-function-like weight functions [55]. Fluid properties and flow boundary conditions arise then as a consequence of the collision dynamics and the local friction controlled by the DPD thermostat. As a matter of fact, as far as one is concerned with the measurement of static contact angles, the particular choice of the thermostat might facilitate the faster equilibration of the system but is otherwise largely irrelevant.

Since the measurement of the contact angle θ for different wettability is our main concern, we vary the wettability by changing the energy parameter ϵ_{LW} of wall-liquid interaction. The interaction of the liquid with the lyophilic part of the slit wall is taken as $\epsilon=1.4$ which guarantees that this part is properly wet up to the pinning line. Beyond the pinning line, the slit is lyophobic due to a purely repulsive interaction with particles of the liquid.

Our basic setup comprises a reservoir connected to a slit with two parallel planes of length $L_y=80$ and width $D=L_z=20$. The planes are at distance $D=20$ from one another. In the present study, we typically deal with 2×10^4 fluid particles. Depending on the slit dimensions and the position of the pinning line, this number may vary significantly.

An essential precondition for the successful application of the method is the existence of zero pressure in the reservoir. Otherwise, any nonnegligible external pressure (including meniscus-induced Laplace pressure in the reservoir) may affect the shape and position of the fluid-vapor interface in the slit and therefore the accuracy of the method. This is achieved by applying *periodic boundary conditions* (PBCs) in z and y directions (see Fig. 1), while in z direction along the slit, we have free boundary conditions with invisible repulsive walls on both sides of the system. Due to the PBC, one creates zero pressure in the reservoir whereby the liquid there stays in equilibrium with its vapor.

IV. WETTING ANGLE DETERMINATION

As a rule, one may determine the contact angle of the fluid with the upper slit wall after the fluid has reached the pinning line and the whole system has attained equilibrium. Depending on the pinning line position, this may take time—according to Lucas-Washburn law of capillary filling [16], the fluid front proceeds as a square root of elapsed time. Some preliminary knowledge about the expected contact angle might help to fix the pinning line position and the amount of fluid particles optimally so as to reduce the time for equilibration. For a quiescent fluid, one may then observe the resulting two-dimensional density profile of the liquid [Figs. 3(a) and 3(b)]. Evidently, in both cases of predominantly lyophilic [Fig. 3(a)] and lyophobic [Fig. 3(b)] upper slit walls, one observes a well-defined fluid-vapor phase boundary. For rather narrow slits, $D=20$, the proximity of the triple phase contact line still induces some curvature of the interface (Fig. 3). For a larger wall separation $D=50$, however, the planar shape of the liquid-phase boundary is evident (Fig. 4).

Apart from the liquid-vapor interface, Fig. 3 displays clearly the effect of liquid layering in the vicinity of the walls. Evidently, the layering effect is better pronounced at wettable walls where ϵ_{LW} is larger.

Even though the resulting contact angles may be directly estimated from the two-dimensional density profiles in the upper graphs of Fig. 3, a much more accurate determination of θ may be achieved if the local position of the interface is established precisely. To this end, one may approximate the crossover from liquid to vapor density at any distance x from the wall by the function

$$\rho[z(x)] = \frac{\rho_L + \rho_V}{2} + \frac{\rho_L - \rho_V}{2}\tanh\left[\frac{x - l(x)}{w_{int}(x)}\right], \tag{19}$$

where ρ_L and ρ_V denote the bulk liquid and vapor densities away from the interface. In Eq. (19), $l(x)$ and $w_{int}(x)$ stand for the local position and width of the interface. This is illustrated by the lower graphs in Fig. 3 and by Fig. 4 where

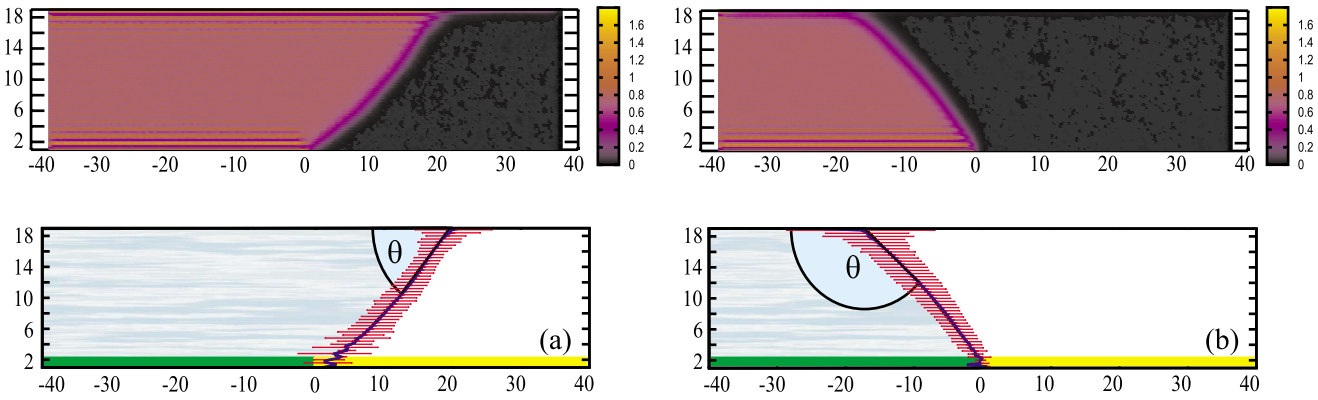

FIG. 3. (Color online) Fluid density profiles (above) and estimated local position and width of the interface for the cases, shown in Fig. 1. The liquid-wall interactions at the upper wall are (a) $\epsilon_{LW}=0.9$ with $\theta=50°\pm2°$ and (b) $\epsilon_{LW}=0.3$ with $\theta=141°\pm2°$. The liquid is pinned in middle of the lower wall at $x=0$.

the blue line locates the interface position while horizontal lines mark the respective $w_{int}^2(x)$.

Our measurements for different slits indicate that θ, which is our main concern in this work, does not depend on the slit size L_y, D. The error in measuring θ is about $\pm1°$. For the typical cases of $\theta=50°\pm2°$ and $\theta=5141°\pm2°$, shown in Fig. 3, one gets the same values also from Fig. 4. Thus, the fraction of straight-line interface, needed for an unambiguous determination of θ, should be a compromise of accuracy and CPU effort.

We have found, however, that the actual interface width perpendicular to the interphase boundary $\bar{w}(\theta)=w_{int}(x)\sin\theta$ slightly but systematically decreases with growing contact angle θ (decreasing wettability) of the wall. We find $\bar{w}(50°)=1.27$, $\bar{w}(90°)=1.30$, and $\bar{w}(141°)=1.32$ if measured close to the three phase contact lines. In contrast to the measured value of θ, we find that $\bar{w}$ may depend on the slit size D, L_y which could be due to line tension effects.

In Fig. 5, we show the change in the contact angle $21°\leq\theta\leq154°$ with varying strength of the liquid-wall interaction ϵ_{LW}. For measuring angles outside this interval, one would need a longer slit and proper positioning of the pinning line. As expected, $\theta\to180°$ when $\epsilon_{LW}\to0$ (entirely lyophobic substrate) while $\theta\to0°$ (complete wetting) when $\epsilon_{LW}\to\epsilon_{LL}$. This θ vs ϵ_{LW} relationship has been already used in a number of studies [18–20] where the knowledge of the contact angle is of crucial importance.

V. SUMMARY

In this work, an efficient method for accurate determination of contact angles between a liquid-vapor interface and a solid surface under conditions of incomplete wetting has been proposed. The method utilizes a setup—a combination of a slit connected to a reservoir with suitable boundary conditions—which produces sufficiently planar liquid-vapor interfaces in the slit and the attached reservoir so that the Laplace pressure in the fluid is eliminated and a reliable tangent to the interface can be drawn. Since the liquid-vapor interface is made to pin on a straight triple contact line, separating a lyophilic from lyophobic part on one of the slit planes, on the second (studied) plane a straight contact line is formed whose length does not depend on the resulting contact angle θ. This guarantees a reliable and accurate determination of θ, free from line tension effects.

The method has been justified theoretically for the case of short-ranged forces between fluid particles and the atoms of the planes using earlier results by Parry *et al.* [54] for the generally adopted effective Hamiltonian [2–8] [Eq. (3)], which determines upon minimization the interface profile in our setup. Eventually, as an example for the proposed method, we have produced a calibrating $\theta-\epsilon$ relationship which relates the observed wetting angle θ to the strength of liquid-wall interactions in a broad interval of values. We believe that both the method as well as the derived $\theta-\epsilon$ dependence may be used in a broad range of related problems pertaining to wetting.

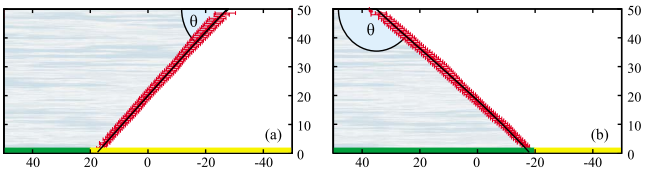

FIG. 4. (Color online) Estimated local position and width of the interface for the cases, shown in Fig. 3 in a wider slit $D=50$. Due to the much larger width D, the pinning line on the lower plane has to be shifted appropriately.

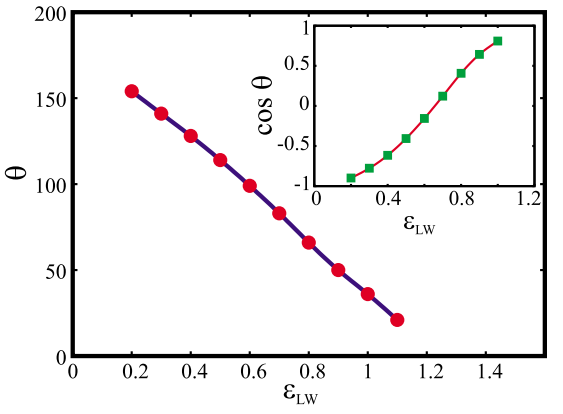

FIG. 5. (Color online) Variations of the contact angle θ (main graph) and cos θ (inset) with changing strength of the wall-liquid interaction ϵ_{LW}.

ACKNOWLEDGMENTS

One of us (A.M.) acknowledges support under Grant No. Bi314/22. Another (D.I.D.) acknowledges support from the Schwerpunkt für Rechengestützte Forschungsmethoden in den Naturwissenschaften (SRFN) during our visit at the University of Mainz, Germany. A.M. and D.I.D. appreciate support by the project "INFLUS," Project No. NMP-031980 of the VI-th FW program of the EC. We are greatly indebted to Professor A. O. Parry for his hint to Ref. [54] and a stimulating discussion.

[1] J. S. Rowlinson and B. Widom, *Molecular Theory of Capillarity* (Clarendon Press, Oxford, 1982).
[2] P.-G. de Gennes, Rev. Mod. Phys. **57**, 827 (1985).
[3] D. E. Sullivan and M. M. Telo da Gamma, in *Fluid Interfacial Phenomena*, edited by C. A. Croxton (Wiley, New York, 1986), p. 45.
[4] S. Dietrich, in *Phase Transitions and Critical Phenomena*, edited by C. Domb and J. L. Lebowitz (Academic Press, New York, 1988), Vol. XII, p. 1.
[5] M. Schick, in *Liquids at Interfaces*, edited by J. Charvolis, J. F. Joanny, and J. Zinn-Justin (North-Holland, Amsterdam, 1990), p. 415.
[6] R. Lipowsky, *Wetting (Physical Chemistry)* (McGraw-Hill, New York, 2000).
[7] D. Bonn and D. Ross, Rep. Prog. Phys. **64**, 1085 (2001).
[8] K. Binder, D. Landau, and M. Müller, J. Stat. Phys. **110**, 1411 (2003).
[9] J.-P. de Gennes, F. Brochard-Wyart, and D. Quere, *Capillary and Wetting Phenomena. Drops, Bubbles, Pearls, Waves* (Springer, Berlin, 2004).
[10] J. F. Joanny, in *Phase Transitions in Soft Condensed Matter*, edited by T. Riste and D. Sherrington (Plenum Press, New York, 1989), p. 221.
[11] D. Quere, Rep. Prog. Phys. **68**, 2495 (2005).
[12] J. De Conninck, M. J. de Ruyter, and M. Voue, Curr. Opin. Colloid Interface Sci. **6**, 49 (2001).
[13] M. Voue and J. De Conninck, Acta Mater. **48**, 4405 (2000).
[14] A. Moosavi, M. Rauscher, and S. Dietrich, Phys. Rev. Lett. **97**, 236101 (2006).
[15] G. Martic, F. Gentner, D. Seveno, J. De Conninck, and T. D. Blake, Langmuir **18**, 7971 (2002).
[16] D. I. Dimitrov, A. Milchev, and K. Binder, Phys. Rev. Lett. **99**, 054501 (2007).
[17] P. Huber, S. Grüner, C. Schäfer, K. Knorr, and A. V. Kityk, Eur. Phys. J. Spec. Top. **141**, 101 (2007).
[18] D. Dimitrov, A. Milchev, and K. Binder, Phys. Chem. Chem. Phys. **10**, 1867 (2008).
[19] F. Diotallevi, S. Chibbaro, E. Costa, D. I. Dimitrov, A. Milchev, D. Palmieri, G. Pontrelli, and S. Succi, Langmuir **25**, 12653 (2009).
[20] S. Chibbaro, L. Biferale, K. Binder, D. Dimitrov, F. Diotallevi, A. Milchev, and S. Succi, J. Stat. Mech.: Theory Exp. **2009**, P06007 (2009).
[21] J. Koplik, J. R. Banavar, and J. F. Willemsen, Phys. Rev. Lett. **60**, 1282 (1988).
[22] N. Giordano and J. T. Cheng, J. Phys.: Condens. Matter **13**, R271 (2001).
[23] A. A. Darhuber, S. M. Troian, and W. W. Reisner, Phys. Rev. E **64**, 031603 (2001).
[24] C. Cottin-Bizonne, S. Jurine, J. Baudry, J. Crassous, F. Restagno, and F. Charlaix, Eur. Phys. J. E **9**, 47 (2002).
[25] M. Cieplak, J. Koplik, and J. R. Banavar, Phys. Rev. Lett. **96**, 114502 (2006).
[26] L. Bocquet and J. L. Barrat, Soft Matter **3**, 685 (2007).
[27] J.-C. Baret, M. Decr, S. Herminghaus, and R. Seemann, Langmuir **23**, 5200 (2007).
[28] M. Rauscher and S. Dietrich, Annu. Rev. Mater. Res. **38**, 143 (2008).
[29] A. C. Zettlemoyer, *Nucleation* (M. Dekker, New York, 1969).
[30] D. Turnbull, J. Appl. Phys. **21**, 1022 (1950); J. Chem. Phys. **18**, 198 (1950).
[31] G. Navascues and P. Taranzona, J. Chem. Phys. **75**, 2441 (1981).
[32] D. Winter, P. Virnau, and K. Binder, Phys. Rev. Lett. **103**, 225703 (2009); J. Phys.: Condens. Matter **21**, 464118 (2009).
[33] T. Young, Philos. Trans. R. Soc. London **85**, 65 (1805).
[34] R. Fondecave and F. Brochard-Wyart, Macromolecules **31**, 9305 (1998).
[35] G. Saville, J. Chem. Soc., Faraday Trans. 2 **73**, 1122 (1977).
[36] P. A. Thompson, W. B. Brinckerhoff, and M. O. Robbins, J. Adhes. Sci. Technol. **7**, 535 (1993).
[37] A. Milchev and K. Binder, J. Chem. Phys. **114**, 8610 (2001).
[38] A. Milchev and A. Milchev, Europhys. Lett. **56**, 695 (2001).
[39] A. Milchev and K. Binder, J. Chem. Phys. **116**, 7691 (2002).
[40] J. Yaneva, A. Milchev, and K. Binder, Macromol. Theory Simul. **12**, 573 (2003).
[41] J. De Coninck and T. D. Blake, Annu. Rev. Mater. Res. **38**, 1 (2008).
[42] L. Boruvka and A. W. Neumann, J. Chem. Phys. **66**, 5464 (1977).
[43] J. O. Indekeu, Int. J. Mod. Phys. B **8**, 309 (1994).
[44] B. Widom, J. Phys. Chem. **99**, 2803 (1995).
[45] D. Li and D. J. Steigmann, Colloids Surf., A **116**, 25 (1996).
[46] T. Bieker and S. Dietrich, Physica A **252**, 85 (1998).
[47] T. Getta and S. Dietrich, Phys. Rev. E **57**, 655 (1998).
[48] M. Brinkmann, J. Kierfeld, and R. Lipowsky, J. Phys.: Condens. Matter **17**, 2349 (2005).
[49] L. Schimmele, M. Napiorkovski, and S. Dietrich, J. Chem. Phys. **127**, 164715 (2007).
[50] R. D. Gretz, J. Chem. Phys. **45**, 3160 (1966).
[51] P. S. Swain and R. Lipowsky, Langmuir **14**, 6772 (1998).
[52] D. Li and A. W. Neumann, Colloids Surf. **43**, 195 (1990).
[53] C. Bauer and S. Dietrich, Eur. Phys. J. B **10**, 767 (1999).
[54] A. O. Parry, E. D. MacDonald, and C. Rascon, J. Phys.: Condens. Matter **13**, 383 (2001).
[55] P. J. Hoogerbrugge and J. M. Koelman, Europhys. Lett. **19**, 155 (1992).
[56] Note that for a homogeneous wall, the solution of $\partial V_{eff}(l)/\partial l|_{l=l_{\min}}=0$ yields $l_{\min}\to\infty$, that is, an infinitely thick wetting layer.